*Desalination and Water Treatment*
www.deswater.com
doi: 10.5004/dwt.2021.27515

233 (2021) 11–18
September

# Purification of tap water to drinking water: nanobubbles technology

C. Rameshkumar[a], G. Senthilkumar[b,*], R. Subalakshmi[c]

[a]*Department of Physics, Sathyabama Institute of Science and Technology, Chennai 600119, India, email: cramkum@gmail.com*
[b]*Department of Mechanical Engineering, Sathyabama Institute of Science and Technology, Chennai 600119, India, email: tosenthilgs79@gmail.com*
[c]*Department of Physics, University of Madras, Chennai – 600 005, Tamil Nadu, India, email: ramsubbu19@gmail.com*

Received 10 October 2020; Accepted 28 May 2021

**ABSTRACT**

This present experimental investigation is focused on arriving at the possibility of drinking water production from tap water irrespective of its quality with nanobubbles (NBs) technology. Out of the two phases in our work, the first phase expresses the generation of NBs and its subsequent substantiation and conversion of this NBs water to drinking water, forms the second phase. The NBs were created by electrolysis in tap water and the same was confirmed with the characterisation studies conducted by scanning electron microscopy and atomic force microscopy. The water quality tests such as chemical oxygen demand (COD), biological oxygen demand (BOD), dissolved oxygen (DO), total dissolved solids (TDS), total suspended solids (TSS), phosphate, chromium and sulphide on the tap water, generated NBs water and purified water after NBs generation ensured the focus of our experimental work. The significant increase in DO %, drastic reduction in BOD, COD, TDS, and TSS confirmed that the above-treated water is a drinkable source. There was a 42.65% increase in DO in water after treatment. There was an abrupt drop of BOD by 50%, COD by 9.5% and TDS by 2.5% due to the removal of scales and dirt.

*Keywords:* Nanobubbles; Aqueous; Atomic force microscopy; Tapping mode; Tap water

## 1. Introduction

Nanobubbles are tiny bubbles with a respective diameter range of 10–50 nm and <200 nm [1], and have been explored for various applications. Water nanobubbles have attracted increasing attention in recent years owing to their extraordinary properties including unexpected prolonged lifetime [2,3], high gas solubility [4], high thermal stability [5] and mechanical strength [6]. The wide application of nanobubbles has been recognized also in many fields, such as biomedicine delivery [7], wastewater treatment [8], non-toxic treatment [9], surface cleaning [10] and befouling membrane [11]. Compared with the macroscopic bubbles, nanobubbles retain for months without bursting out at once as the large bubble does [12]. Nanobubbles at the surface were dynamically stable [13] as revealed by atomic force microscopy (AFM) investigation; Monolayer water can make the surface nanobubbles stable [14]. The stability of nanobubbles was considered as arising from the low gas diffusion through the water, or from the pinned contact water surface of the nanobubbles, as suggested by theoretical investigations [15]. Nanobubbles had a slow dissolution rate for hours or up to days, compared with the microsecond's lifetime for macroscopic bubbles [16]. Nanobubbles have an unexpected large contact angle and high surface tension [17]. Nanobubbles are defined by their diameter – less than one micron and larger than a nanometre [18]. However, the most distinguishing feature of nanobubbles is longevity [19]. This longevity has two aspects [20]. The virtual disappearance of the buoyant force is the most prominent or the obvious one [21]. Bubbles that are smaller than 5 microns in diameter do not rise to the top surface [22]. Since the buoyant force is smaller than

* Corresponding author.

any current in the liquid, it can also be flooded by the repulsive forces of these types of bubbles with each other and also with the other interactive forces [23]. The second less obvious aspect of longevity is physical stability [24], (i.e., such bubbles do not dissolve away). They are a heterogeneity that is preserved, much like imperfections in a crystalline structure. The activities of the liquid molecules are readjusted in such a way, that they take place without any interference with the heterogeneous regime. Nanobubbles, once formed, are highly persistent. This is both a blessing and a curse [25]. If energy-efficient, low-cost nanobubbles are available, the commodity applications where many bubbles are found to be dependent on the existence of the "permanent" heterogeneity in the liquid at the uniformly dispersed nanobubbles sited [26,27]. As the bubbles rise up to the surface, they latch onto the solids (contaminants) that are suspended in the liquid and carry them up to the surface [28]. As these suspended solids are not constant in size and shape, the larger bubbles often fail to latch onto them and end up incapable of bringing them up to the surface, but nanobubbles, being very minute in size are capable of holding and latching onto them from all the sides, and because of free radicals promote the process of floatation of these suspended solids. The generation procedures of nanobubbles (NBs) were hydrodynamic cavitation, temperature exchange method, ultrasonication and electrolysis. In our experimental work, the NBs were generated in domestic tap water by electrolysis with a voltage range of 8–12 V and subjected to purification by reverse osmosis. The observed NBs were very flat and had radii of the order of 50 nm at the surface and a height of 10 nm, which yielded a low contact angle. The presence of NBs was confirmed from the characterization of scanning electron microscopy (SEM) and AFM. The aqueous was subjected to various quality tests such as chemical oxygen demand (COD), biological oxygen demand (BOD), dissolved oxygen (DO), total dissolved solids (TDS), total suspended solids (TSS), phosphate, chromium and sulphide before and after the presence of NBs. This current research includes the physics in methods of generation of NBs while production of free radicals from NBs was reviewed with the focus on the degradation of toxic compounds, water disinfection, and cleaning/befouling of solid surfaces and a steady-state approach issued to study the stability of surface nanobubbles in water electrolysis. The electrolysis process is used for generating nanobubbles, which are capable of breaking organic waste with the help of free radicals. To detect the presence of nanobubbles in the water AFM had been done, which was helpful to know the different shapes and sizes of nanobubbles, and further this is made to pass through a set up where the dirt is finally removed and can be consumed, which is considered to be much more beneficial. The obtained results with the treated aqueous have given good agreement with the existing experimental evidence.

## 2. Generation and substantiation of NBs

The 5 L of tap water was electrolysed for the production of ultra-fine NBs for a duration of 60 min as described by authors in their previous publication in Desalination and Water Treatment Journal. The size of NBs as revealed by AFM is presented in Fig. 1 with a scan size of 5 μm × 5 μm.

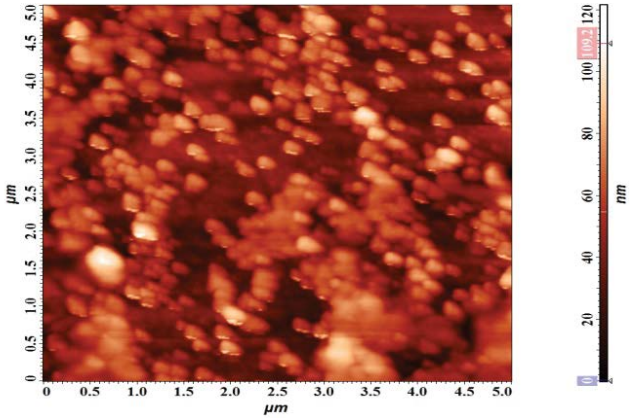


Fig. 1. AFM image of NBs with scan size 5 μm × 5 μm.

The topography synthesis of NBs was characterized by AFM analysis. In AFM, the surface was imaged based on sensing interacting forces between atoms of a sharp tip mounted on a flexible cantilever and atoms of the sample. During the measurement, depending on the microscope model, the cantilever and the tip were lowered towards the sample or the sample was lifted towards the tip until the contact was made. The displacement of the cantilever was detected through a laser beam reflected from the top side of the cantilever onto a photodetector. The 3-D image of NBs is given in Fig. 2 with uniform distribution of NBs throughout the aqueous solution. It was also an outcome that the NBs concentration was in inverse proportion with the NBs size.

The surface roughness also increases with the presence of NBs which influences the longevity of NBs. The size distribution of generated NBs is depicted in Fig. 3.

The cantilever was moved in a certain way over the sample (usually lines) and the information over the surface was gathered. The histogram of the average size of the nanobubbles throughout the specimen is represented in Fig. 4.

The spatial resolution depends on the tip shape and the microscope model but is in the nanometre range. With

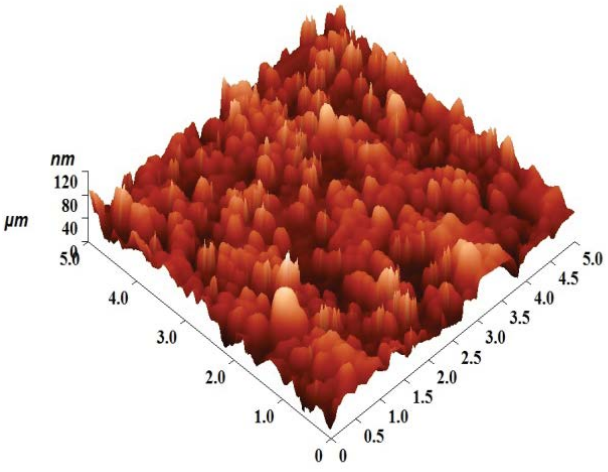


Fig. 2. 3-D image of NBs.

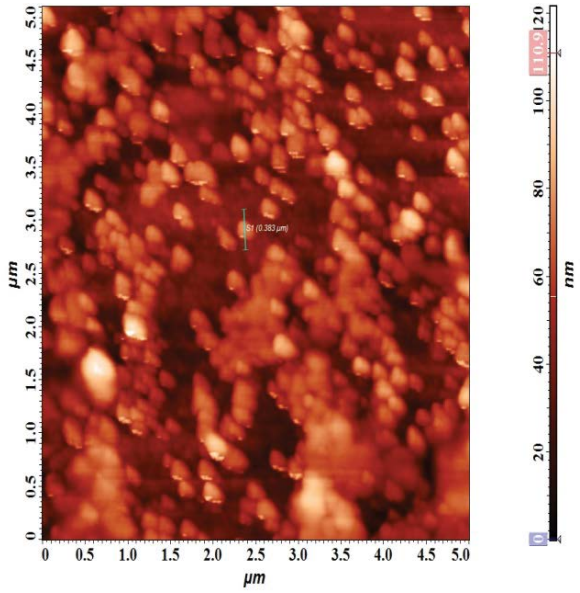


Fig. 3. Surface roughness of NBs.

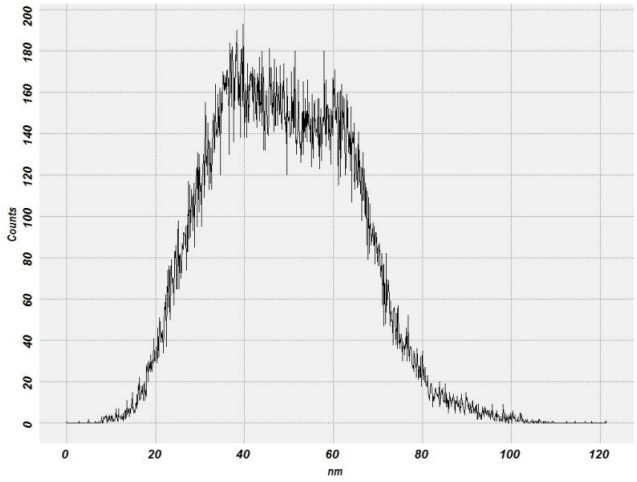


Fig. 4. Histogram of the average size of the NBs.

proper calibration, changes in the voltage are transformed into changes in the sample topography or other parameters. The AFM image of the NBs scan-line at X section at 2,430 nm with bubble size 124 nm is provided in Fig. 5.

So far, a number of imaging modes were employed to study surface nanobubbles. They were based on different principles, operate in different force regimes and were able to provide different information about the sample. Fig. 6 shows the AFM histogram line for the X section at 2,430 nm with bubble size 124 nm.

The AFM image of the NBs scan-line at X section at 3,820 nm with bubble size 195 nm is indicated in Fig. 7.

In the tapping mode (TM) AFM contrary, to contact mode, in TM imaging, the cantilever was oscillated at (or close to) its resonance frequency with an amplitude A. The AFM histogram line for the X section at 3,820 nm with bubble size 195 nm is illustrated in Fig. 8.

When the tip is far from the sample surface, $A$ is equal to the free (maximum) amplitude $A_o$. When the tip is lowered towards the sample during a topographic scan, $A_o$ is damped by the interaction forces between the tip apex and the surface. In the vicinity of the surface, the amplitude is

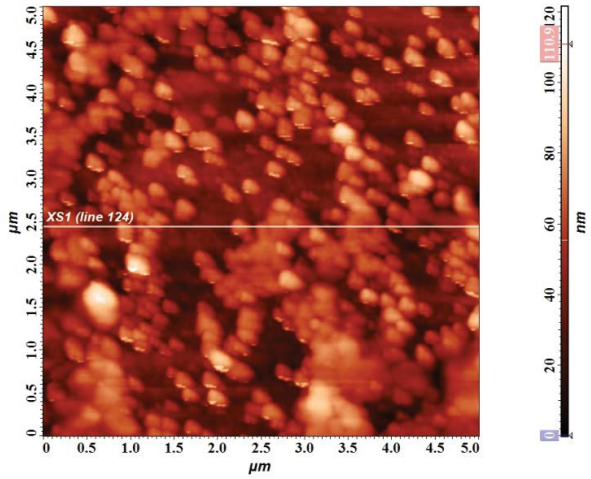


Fig. 5. AFM image of the NBs scan-line at X section at 2,430 nm with bubble size 124 nm.

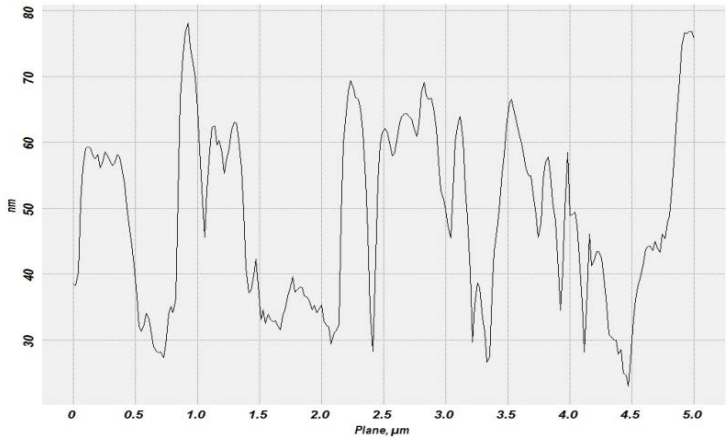


Fig. 6. AFM histogram line for X section at 2,430 nm with bubble size 124 nm.

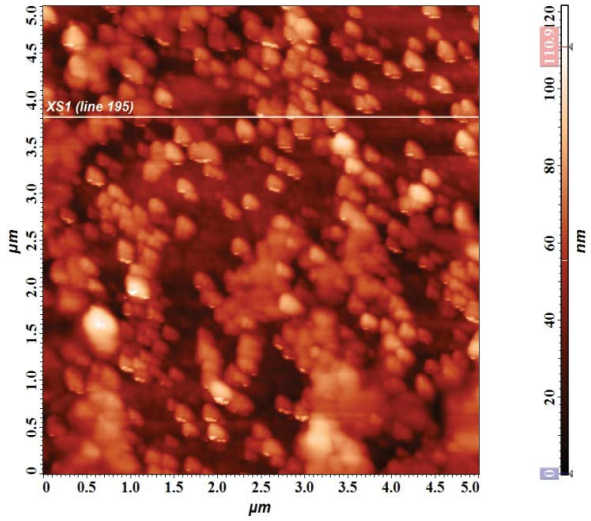


Fig. 7. AFM image of the NBs scan-line at X section at 3,820 nm with bubble size 195 nm.

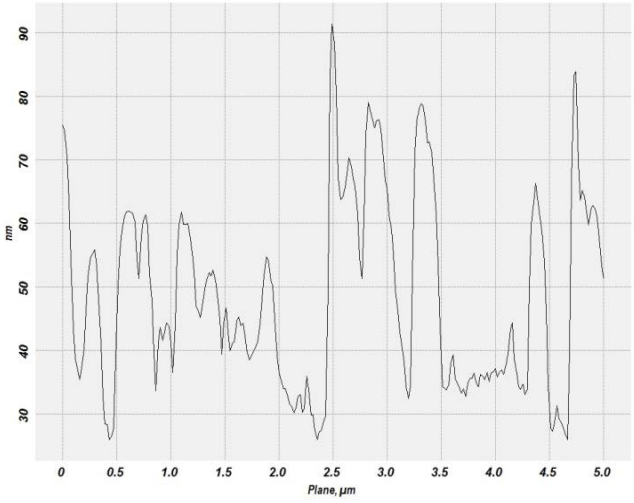


Fig. 8. AFM histogram line for X section at 3,820 nm with bubble size 195 nm.

decreased to a minimum (zero). In a particular taping mode experiment, the extent of damping of the oscillation upon establishing "contact" with the surface is defined by set-point amplitude. As per the set-point ratio ($A_{sp}/A_0$) × 100%. In general, a large set-point value means smaller damping and, because the amplitude and the force dependences are related, it also means smaller force exerted on the sample and experienced by the tip.

## 3. Result and discussion

### 3.1. Substantiation by SEM

The SEM is considered to be a variant in the study of the electron microscopy that emits images of the given specific sample by scanning the outer surface with a focused beam of electrons. The electrons that have been focussed on the surface of the sample then interact with atoms present on it, thus producing various signals that possess information about the surface topography, structure of atoms and composition of the sample. For testing the presence of nanobubbles in the water, a sample of 2.5 mL was taken. From that, only a single drop was taken on a glass slide and subject to dry in room temperature. Once the sample was dried in room temperature, it was taken for gold sputtering (as it is a non-conductive sample). After the completion of the sputtering, the sample was taken for AFM and SEM testing, and the following results were obtained.

Thus the roughness analysis for the considered specimen of nanobubble for 5 μm × 5 μm was found out to be,

| | |
|---|---|
| Amount of sampling | 655,36 |
| Maximum | 121.434 nm |
| Minimum | 0 nm |
| Peak-to-peak, Sy | 121.434 nm |
| Ten point height, Sz | 60.9279 nm |
| Average | 48.7289 nm |
| Average roughness, Sa | 13.06 nm |
| Root mean square, Sq | 15.8166 nm |
| Second moment | 2,624.68 |
| Surface skewness, Ssk | 0.262938 |
| Coefficient of kurtosis, Ska | –0.300199 |
| Entropy | 9.15737 |
| Redundance | –0.324832 |

From the above AFM results, numerous nanobubbles were found, that were created using the electrolysis process. A smaller part of the area was scanned by tapping mode in AFM. This model revealed the presence of nanobubbles in the scanning area of 5 μm × 5 μm. The average size of the nanobubbles for the considered area in the specimen was found to be 48.7289 nm. The SEM image of the nanobubbles scan-line is given in Fig. 9.

Fig. 10 shows the SEM image of the nanobubbles scan-line at different places of the sample is considered with the surface morphology.

The SEM image of the nanobubbles scan-line at a specific place of the sample is considered is represented in Fig. 11.

The SEM also provides the size distribution of NBs over the entire surface of the aqueous. The SEM image of the nanobubbles scan-line at a specific place with a different magnification factors of the sample is considered is given in Fig. 12.

The image of the sample that was taken for testing nanobubble's presence in the given test sample is observed in Fig. 13.

### 3.2. NBs water quality test after purification

The tap water is taken directly into the tank, nearly 5 L of water is taken for the treatment process. The water from the inlet then passes through the nanobubble generating system, which was kept in operation for a necessary time period. Once the nanobubbles start generating, the water appears to be cloudy; indicating the presence of nanobubbles and the free radicals generated in the process after the operation is stopped. As soon as the process is stopped, the sludge that reaches the surface as a result

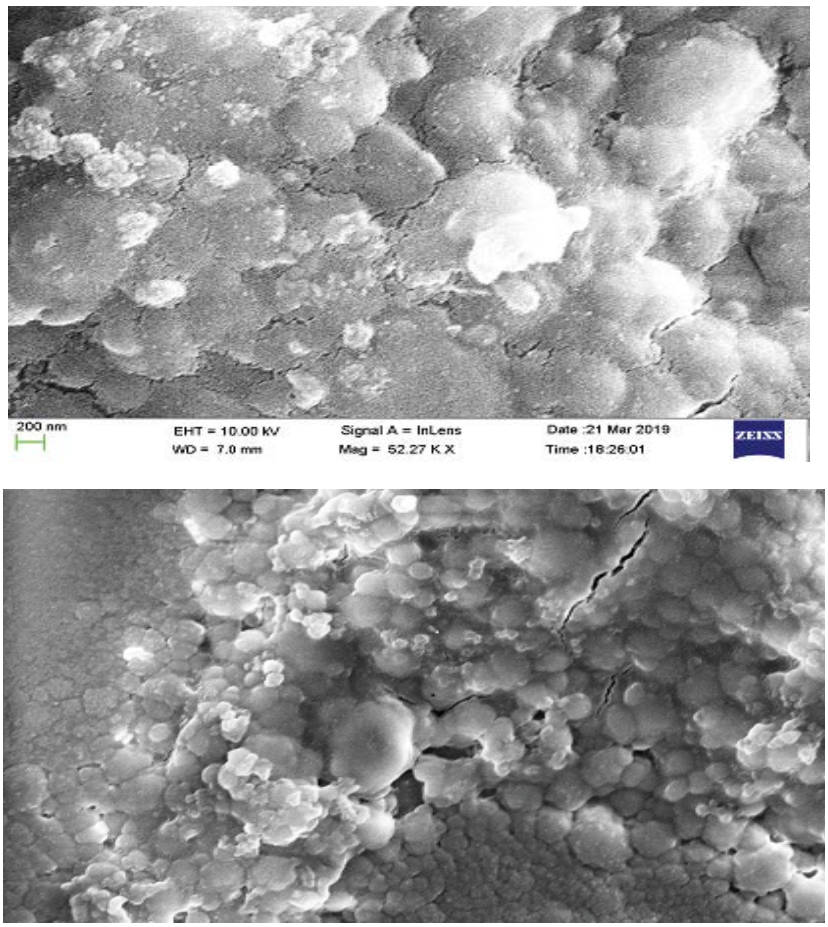


Fig. 9. SEM image of the NBs scan-line.

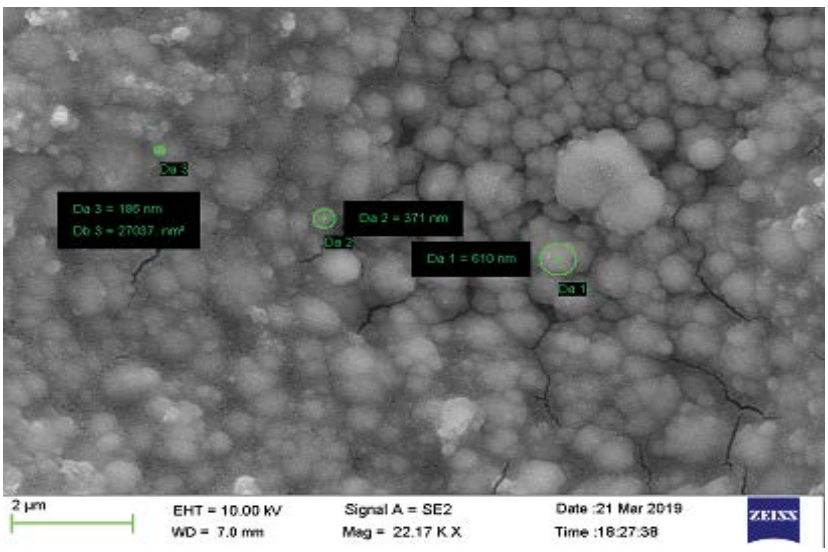


Fig. 10. SEM image of the NBs scan-line at different places of the sample is considered.

of the flocculation is then pumped out immediately without any loss of time, as it starts to settle as time passes by. Once the dirt is pumped out from the top, the remaining water is made to pass through a purification process and then the end water sample that is obtained is further taken to the lab, for testing the water quality before and after treatment by measuring different parameters which shows the effect of nanobubbles before and after

treatment by giving us positive results, initially, that is before treatment the BOD, COD, DO, TSS, TDS and phosphates contain was more and after treatment we can see the quality of water had improved from bad to good, if we take a look on Table 2, we can compare the values of different parameters, before the treatment COD level was 11 mg/L which has decreased to BDL (below detection limit)/DL (detection limit) 4 mg/L, same can be explained for BOD, as decreased in the BOD level increases the oxygen level in the tap water after treatment, likewise all the parameters have given positive results after the treatment.

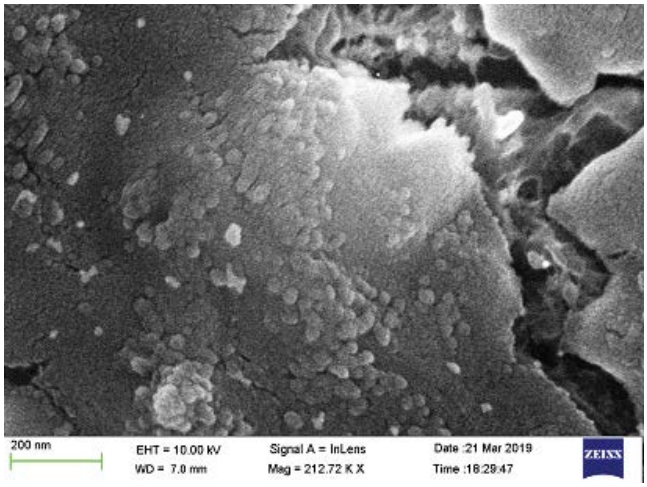


Fig. 11. SEM image of the NBs scan-line at a specific place of the sample is considered.

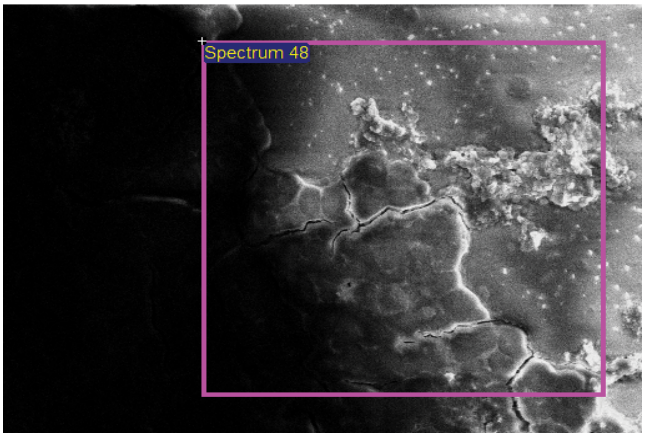


Fig. 13. Image of the sample that was taken for testing NBs presence in the given test sample.

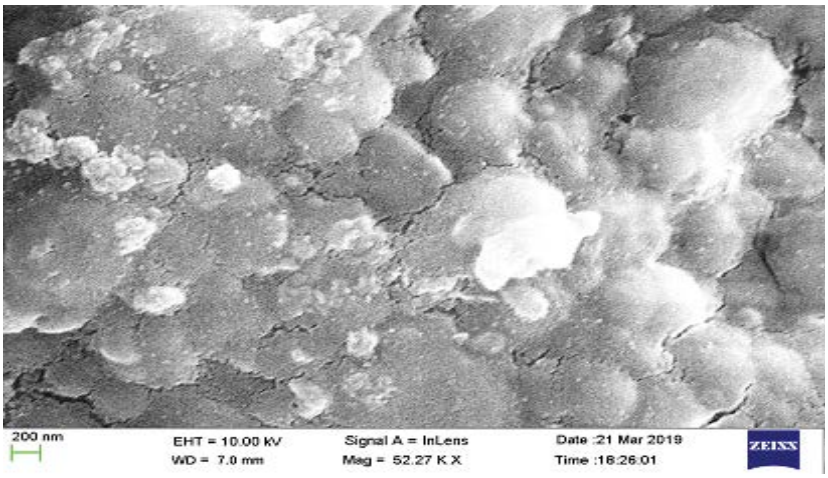


Fig. 12. SEM image of the NBs scan-line at a specific place with a different magnification factors of the sample is considered.

Table 1
Water quality enhancement after treatment

| Sl. No. | Parameters | Before (mg/L) | After electrolysis (mg/L) | Final product from specimen (mg/L) |
|---|---|---|---|---|
| 1 | BOD | 4 | 2 | BDL(DL:2.0) |
| 2 | COD | 21 | 19 | 6.3 |
| 3 | DO | 6.8 | 9.7 | 6.7 |
| 4 | TDS | 1,302 | 1,269 | 1,286 |
| 5 | TSS | 12 | 24 | BDL(DL:1.0) |
| 6 | Phosphate | 22.5 | 0.14 | 0.36 |
| 7 | Chromium | 0.049 | 0.366 | BDL(DL:0.005) |
| 8 | Sulphide | BDL(DL:0.01) | BDL(DL:0.01) | BDL(DL:0.01) |

Table 2
Thermophysical properties of NBs water with microconstituents

| Test | Protocol | Results | Limits as per IS 10500:2012, with Amendment No. 2 | |
|---|---|---|---|---|
| | | | Acceptable limit (max.) | Permissible limit in absence of alternate source (max.) |
| Colour | IS: 3025: Part:4-1983 (Reaff:2012) | 5 Hazen | 5 | 15 |
| Odour | IS: 3025: Part:5-1983 (Reaff:2012) | Agreeable | Agreeable | Agreeable |
| pH at 25°C | IS: 3025: Part:11-1983 (Reaff:2012) | 7.49 | 6.5–8.5 | 6.5–8.5 |
| Conductivity at 25°C | IS: 3025: Part:14-2013 | 1,929 μm hos/cm | – | – |
| Total dissolved solids | IS: 3025: Part:16-1984 (Reaff:2012) | 1,061 mg/L | 500 mg/L | 2,000 mg/L |
| Total hardness as $CaCo_3$ | IS: 3025: Part:21-2009 (Reaff:2014) | 280 mg/L | 200 mg/L | 600 mg/L |
| Calcium as Ca | IS: 3025: Part:40-1991 (Reaff:2014) | 55 mg/L | 75 mg/L | 200 mg/L |
| Magnesium as Mg | IS: 3025: Part:46-1994 (Reaff:2014) | 35 mg/L | 30 mg/L | 100 mg/L |
| Chloride as Cl | IS: 3025: Part:32-1988 (Reaff:2014) | 347 mg/L | 250 mg/L | 1,000 mg/L |
| Total alkalinity as $CaCo_3$ | IS: 3025: Part:23-1986 (Reaff:2014) | 246 mg/L | 200 mg/L | 600 mg/L |
| Sulphate as $SO_4$ | IS: 3025: Part:24-1986 (Reaff:2014) | 78 mg/L | 200 mg/L | 400 mg/L |
| Nitrate as $NO_3$ | IS: 3025: Part:34-1988 (Reaff:2014) | 5 mg/L | 45 mg/L | 45 mg/L |
| Iron as Fe | IS: 3025: Part:53-2003 (Reaff:2014) | 1.43 mg/L | 1.0 mg/L | 1.5 mg/L |
| Fluoride as F | APHA-22nd ed. 2012-4500 F,D | 0.33 mg/L | 1.0 mg/L | 1.5 mg/L |
| *Escherichia coli* | #IS: 15185-2016 | Absent/100 mL | Shall not be detected in any 100 mL sample | |
| Total coliform | #IS: 15185-2016 | Absent/100 mL | | |

In this study, the water quality test was carried out using standard methods for the examination of tap water and is listed in Table 1. In this study, one case study demonstrated the efficiency of inducing nanobubbles in tap water and can be considered to be consumed by humans. This case study used one type of water source, which is tap water.

The thermophysical properties with microconstituents before and after the presence of NBs is given in Table 2.

## 4. Conclusions

The generated NBs by electrolysis were effectively utilized for the treatment of aqueous and the following conclusions were made. The generated NBs were with an average size of 100–200 nm as revealed from AFM. It was apparent that there was a strong swell of 42.65% in DO in water after treatment. There was an abrupt drop of BOD by 50%, COD by 9.5% and TDS by 2.5% due to the removal of scales and dirt. Almost all the microconstituents present in NBs treated aqueous were within the acceptable limits. Hence it is suggested that NBs technology can be utilized for aqueous treatment without much drawbacks. This experimental study comes up with that the aqueous to be cast-off in further exploration and industrial research. Our future NBs work will be extended to drug discovery, cancer treatment, agriculture, aquaculture and combustion phenomenon in I.C. engines.

## Acknowledgment

We thank International Research Centre (IRC), Sathyabama Institute of Science and Technology, IIT Madras, Chennai and Chennai Mettex Lab Pvt. Ltd. for carrying our research in this pandemic period.

## References

[1] A. Agarwal, W.J. Ng, Y. Liu, Principle and applications of microbubble and nanobubble technology for water treatment, Chemosphere, 84 (2011) 1175–1180.
[2] C.U. Chan, M. Arora, C.-D. Ohl, Coalescence, growth, and stability of surface-attached nanobubbles, Langmuir, 31 (2015) 7041–7046.
[3] H. Rezaei Nejad, M. Ghassemi, S.M. Mirnouri Langroudi, A. Shahabi, A molecular dynamics study of nanobubble surface tension, Mol. Simul., 37 (2011) 23–30.
[4] J.H. Weijs, D. Lohse, Why surface nanobubbles live for hours, Phys. Rev. Lett., 110 (2013) 054501, doi: 10.1103/PhysRevLett.110.054501.
[5] J.R.T. Seddon, D. Lohse, W.A. Ducker, V.S.J. Craig, A deliberation on nanobubbles at surfaces and in bulk, ChemPhysChem, 13 (2012) 2179–2187.
[6] L. Luo, H.S. White, Electrogeneration of single nanobubbles at sub-50-nm-radius platinum nanodisk electrodes, Langmuir, 29 (2013) 11169–11175.
[7] L.J. Zhang, Y. Zhang, X.H. Zhang, Z.X. Li, G.X. Shen, M. Ye, C.H. Fan, H.P. Fang, J. Hu, Electrochemically controlled formation and growth of hydrogen nanobubbles, Langmuir, 22 (2009) 8109–8113.
[8] P. Li, M. Takahashi, K. Chiba, Enhanced free-radical generation by shrinking microbubbles using a copper catalyst, Chemosphere, 77 (2009) 1157–1160.
[9] G.M. Liu, Z.H. Wu, V.S.J. Craig, Cleaning of protein-coated surfaces using nanobubbles: an investigation using a quartz crystal microbalance, J. Phys. Chem. C, 112 (2008) 16748–16753.
[10] G. Senthilkumar, C. Rameshkumar, M.N.V.S. Nikhil, J. Navin Ram Kumar, An investigation of nanobubbles in aqueous solutions for various applications, Appl. Nanosci., 8 (2018) 1557–1567.

[11] C. Rameshkumar, G. Senthilkumar, R. Subalakshmi, R. Gogoi, Generation and characterization of nanobubbles by ionization method for wastewater treatment, Desal. Water Treat., 164 (2019) 98–101.
[12] M. Matsumoto, K. Tanaka, Nano bubble—size dependence of surface tension and inside pressure, Fluid Dyn. Res., 40 (2008) 546–553.
[13] B.E. Oeffinger, M.A. Wheatley, Development and characterization of a nano-scale contrast agent, Ultrason. Langmuir, 42 (2004) 343–347.
[14] M. Sumikura, M. Hidaka, H. Murakami, Y. Nobutomo, T. Murakami, Ozone micro-bubble disinfection method for wastewater reuse system, Water Sci. Technol., 56 (2007) 53–61.
[15] S.J. Yang, P.C. Tsai, E. Stefan Kooij, A. Prosperetti, H.J.W. Zandvliet, D. Lohse, Electrolytically generated nanobubbles on highly orientated pyrolytic graphite surfaces, Langmuir, 25 (2009) 1466–1474.
[16] S. Wang, M.H. Liu, Y.M. Dong, Understanding the stability of surface nanobubbles, J. Phys. Condens Matter., 25 (2013) 184007, doi: 10.1088/0953-8984/25/18/184007.
[17] X.H. Zhang, N. Maeda, V.S.J. Craig, Physical properties of nanobubbles on hydrophobic surfaces in water and aqueous solutions, Langmuir, 22 (2006) 5025–5035.
[18] C. Rameshkumar, S. Lakshmi Sankar, G. Senthilkumar, Characterisation of seed germination using nanaobubbled water, Int. J. Ambient Energy, (2019) (in Press), doi: 10.1080/01430750.2019.1672581.
[19] S. Gobinath, G. Senthilkumar, N. Beemkumar, Air nanobubble-enhanced combustion study using mustard biodiesel in a common rail direct injection engine, Energy Sources Part A, 41 (2018) 1809–1816.
[20] S. Mozaffar, P. Tchoukov, A. Mozaffar, J. Atias, J. Czarnecki, N. Nazemifar, Capillary driven flow in nanochannels – application to heavy oil rheology studies, Colloids Surf., A, 513 (2017) 178–187.
[21] S. Mozaffari, P. Tchoukov, J. Atias, J. Czarnecki, N. Nazemifard, Effect of asphaltene aggregation on rheological properties of Diluted Athabasca Bitumen, Energy Fuels, 29 (2015) 5595–5599.
[22] Z.G. Zheng, X.C. Zhang, D. Carbo, C. Clark, C.-A. Nathan, Y. Lvov, Sonication assisted synthesis of polyelectrolyte coated curcumin nanoparticles, Langmuir, 26 (2010) 7679–7681.
[23] Y.M. Lvov, P. Pattekari, X.C. Zhang, V. Torchilin, Converting poorly soluble materials into stable aqueous nanocolloids, Langmuir, 27 (2011) 1212–1217.
[24] P. Pattekari, Z. Zheng, X. Zhang T. Levchenko, V. Torchilin, Y. Lvov, Top-down and bottom-up approaches in production of aqueous nanocolloids of low solubility drug paclitaxel, Phys. Chem. Chem. Phys., 13 (2011) 9014–9019.
[25] A.F. Alghannam, Metabolic limitations of performance and fatigue in football, Asian J. Sports Med., 4 (2012) 65–73.
[26] D. Vergara, C. Bellomo, X.C. Zhang, V. Vergaro, A. Tinelli, V. Lorusso, R. Rinaldi, Y.M. Lvov, S. Leporatti, M. Maffia, Lapatinib/Paclitaxel polyelectrolyte nanocapsules for overcoming multidrug resistance in ovarian cancer, Nanomedicine: NBM, 8 (2012) 891–899.
[27] V. Vergaro, F. Scarlino, C. Bellomo, R. Rinaldi, D. Vergara, M. Maffia, F. Baldassarre, G. Giannelli, X.C. Zhang, Y.M. Lvov, S. Leporatti, Drug-loaded polyelectrolyte microcapsules for sustained targeting of cancer cells, Adv. Drug Delivery Rev., 63 (2011) 847–864.
[28] G. Senthilkumar, M. Purusothaman, C. Rameshkumar, N. Joy, S. Sachin, K. Siva Thanigai, Generation and characterization of nanobubbles for heat transfer applications, Mater. Today:. Proc., 43 (2021) 3391–3393.